

Supplementary Material of URetinex-Net: Retinex-based Deep Unfolding Network for Low-light Image Enhancement

Wenhui Wu¹ Jian Weng² Pingping Zhang³ Xu Wang^{2*} Wenhan Yang⁴ Jianmin Jiang²

¹College of Electronics and Information Engineering, Shenzhen University

²College of Computer Science and Software Engineering, Shenzhen University

³Department of Computer Science, City University of Hong Kong

⁴School of Electrical and Electronic Engineering, Nanyang Technological University

Abstract

This is the supplementary material for the paper: “URetinex-Net: Retinex-based Deep Unfolding Network for Low-light Image Enhancement” submitted to the CVPR 2022. We first demonstrate details of the derivation of our closed-form solution. Besides, we present visual effects on the unfolding process. Next, we evaluate efficiency in terms of performance and speed compared with State-of-the-Arts (SOTA). Finally, we report more qualitative analysis on three real-world datasets, including LOL dataset, SICE dataset and MEF dataset.

A. Derivation of closed-form solution

This section provide complete derivation of closed-form solution to the “**Updating rules for P and Q** ” described in **Sec. 3.2.2** of our submitted paper.

P -subproblem. By differentiating Eq. (5) with respect to P and setting derivative to 0, we have

$$\frac{\partial(\|I - P \cdot Q_{k-1}\|_F^2 + \gamma\|P - R_{k-1}\|_F^2)}{\partial P} = 0. \quad (19)$$

By using $\|P\|_F^2 = \text{Tr}(PP^T)$, Eq. (19) is reformed into:

$$\begin{aligned} & \frac{\partial[\text{Tr}((I - P \cdot Q_{k-1})(I - P \cdot Q_{k-1})^T) + \gamma\|P - R_{k-1}\|_F^2]}{\partial P} \\ & = 0, \end{aligned} \quad (20)$$

where $\text{Tr}(\cdot)$ denotes trace of a matrix. Therefore, we can obtain the following equation:

$$P \cdot Q_{k-1} \cdot Q_{k-1} - I \cdot Q_{k-1} + \gamma(P - R_{k-1}) = 0. \quad (21)$$

Thus, the closed-form solution to P -subproblem in Eq. (5) can be derived as

$$P_k = \frac{\gamma R_{k-1} + I \cdot Q_{k-1}}{Q_{k-1} \cdot Q_{k-1} + \gamma \mathbf{1}}, \quad (22)$$

where $\mathbf{1}$ denotes all-ones matrix.

Q -subproblem. Similarly, by differentiating Eq. (12) with respect to Q and setting derivative to 0, we have

$$\sum_{c \in \{R, G, B\}} (Q \cdot P_k^{(c)} \cdot P_k^{(c)} - I^{(c)} \cdot P_k^{(c)}) + \lambda(Q - L_{k-1}) = 0. \quad (23)$$

Finally, the closed-form solution with regard to Q -subproblem can be derivated as:

$$Q_k = \frac{\lambda L_{k-1} + \sum_{c \in \{R, G, B\}} I^{(c)} \cdot P_k^{(c)}}{\sum_{c \in \{R, G, B\}} P_k^{(c)} \cdot P_k^{(c)} + \lambda \mathbf{1}}. \quad (24)$$

B. Visual effect on unfolding process

As shown in Fig. 1, we provide a visual effect of our unfolding process to illustrate the advantage of our proposed URetinex-Net. Apparently, heavy noise distortion is appeared on the initial reflectance layer R_0 . Through updating in each stage, noise in reflectance is suppressed while details are preserved, which indicates the superiority of our unfolding optimization. Meanwhile, illumination becomes smoother as the number of stage increases.

C. Efficiency evaluation

Next, we evaluate efficiency in terms of PSNR and running speed on LOL datasets compared with SOTA methods. As illustrated in Fig. 2, URetinex-Net performs much better than other methods in PSNR. Moreover, our method runs faster than traditional model-based methods, which suffer

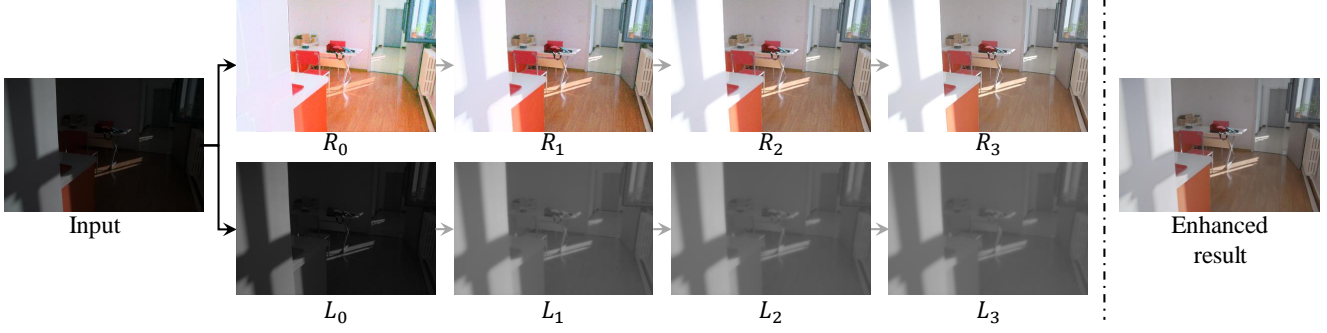


Figure 1. Visual effects of the unfolding process. The reflectance layer step-wise gets rid of noise degradation, while illumination layer becomes smoother stage by stage. Noted that gamma correction is adopted to illumination layers (L_1 , L_2 and L_3) for better visual effects.

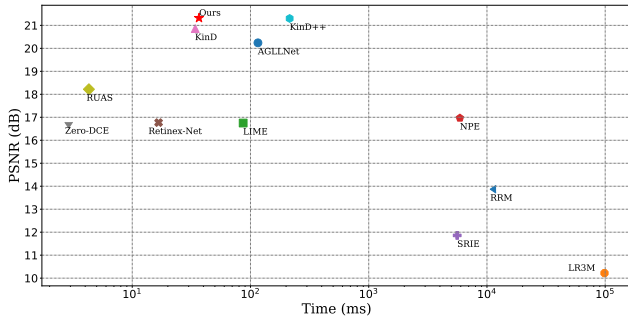


Figure 2. Efficiency evaluation in terms of average values of PSNR and running time on LOL dataset. Log-scale is used on the x-axis for illustration.

from time-consuming iterative optimization procedures, especially RRM, which incorporate noise terms for noise suppression. Although Zero-DCE and RUAS have fast processing speeds, they have limited capacity to reach satisfactory visual results. In summary, taking both computational efficiency and visual performance into account, the proposed URetinex-Net shows promising superiority.

D. Qualitative analysis

In our submitted paper, we have provided sufficient quantitative results (Table 1) and parts of visual comparisons (Figs. 5-6) due to the limit of space. Here, we provide more qualitative analysis compared with all SOTA methods, including LIME [3], NPE [8], SRIE [1], LR3M [7], RRM [4], Retinex-Net [9], KinD [11], Zero-DCE [2], KinD++ [10], AGLNet [6] and RUAS [5]. Figs. 3-5 demonstrate the enhanced results on LOL datasets. Specifically, most comparison methods suffer from heavy noise, including traditional model-based methods, Retinex-Net and ZeroDCE. KinD, KinD++ and RUAS adopt the post-processing denoising operations to further restore results, but it may lead to a loss of details or unnatural looks. Moreover, RUAS has the risk of over-exposure due to the ig-

norance of reflectance during decomposition. In general, our URetinex-Net is capable of noise suppression and detail preservation, demonstrating its superiority over SOTA methods.

Furthermore, we show extensive results to validate the generalisation performance of our proposed URetinex-Net without retraining or fine-tuning. Figs. 6-8 show the visual results on three different scenes in SICE dataset. Obviously, our URetinex-Net is robust to handle artifact distortion and over-exposure, which demonstrates generalization ability of URetinex-Net. Finally, we give complete comparison on MEF dataset in Figs. 9-11.

References

- [1] Xueyang Fu, Delu Zeng, Yue Huang, Xiao-Ping Zhang, and Xinghao Ding. A weighted variational model for simultaneous reflectance and illumination estimation. In *Proceedings of the IEEE conference on computer vision and pattern recognition*, pages 2782–2790, 2016. 2
- [2] Chunle Guo, Chongyi Li, Jichang Guo, Chen Change Loy, Junhui Hou, Sam Kwong, and Runmin Cong. Zero-reference deep curve estimation for low-light image enhancement. In *Proceedings of the IEEE/CVF Conference on Computer Vision and Pattern Recognition*, pages 1780–1789, 2020. 2
- [3] Xiaojie Guo, Yu Li, and Haibin Ling. Lime: Low-light image enhancement via illumination map estimation. *IEEE Transactions on image processing*, 26(2):982–993, 2016. 2
- [4] Mading Li, Jiaying Liu, Wenhan Yang, Xiaoyan Sun, and Zongming Guo. Structure-revealing low-light image enhancement via robust retinex model. *IEEE Transactions on Image Processing*, 27(6):2828–2841, 2018. 2
- [5] Risheng Liu, Long Ma, Jiaao Zhang, Xin Fan, and Zhongxuan Luo. Retinex-inspired unrolling with cooperative prior architecture search for low-light image enhancement. In *Proceedings of the IEEE/CVF Conference on Computer Vision and Pattern Recognition*, pages 10561–10570, 2021. 2
- [6] Feifan Lv, Yu Li, and Feng Lu. Attention guided low-light image enhancement with a large scale low-light simulation dataset. *International Journal of Computer Vision*, 129(7):2175–2193, 2021. 2

- [7] Xutong Ren, Wenhan Yang, Wen-Huang Cheng, and Jiaying Liu. Lr3m: Robust low-light enhancement via low-rank regularized retinex model. *IEEE Transactions on Image Processing*, 29:5862–5876, 2020. 2
- [8] Shuhang Wang, Jin Zheng, Hai-Miao Hu, and Bo Li. Naturalness preserved enhancement algorithm for non-uniform illumination images. *IEEE Transactions on Image Processing*, 22(9):3538–3548, 2013. 2
- [9] Chen Wei, Wenjing Wang, Wenhan Yang, and Jiaying Liu. Deep retinex decomposition for low-light enhancement. *arXiv preprint arXiv:1808.04560*, 2018. 2
- [10] Yonghua Zhang, Xiaojie Guo, Jiayi Ma, Wei Liu, and Jiawan Zhang. Beyond brightening low-light images. *International Journal of Computer Vision*, 129(4):1013–1037, 2021. 2
- [11] Yonghua Zhang, Jiawan Zhang, and Xiaojie Guo. Kindling the darkness: A practical low-light image enhancer. In *Proceedings of the 27th ACM international conference on multimedia*, pages 1632–1640, 2019. 2



Figure 3. Visual comparison on LOL dataset #22 with SOTA LLIE methods.



Figure 4. Visual comparison on LOL dataset #79 with SOTA LLIE methods.

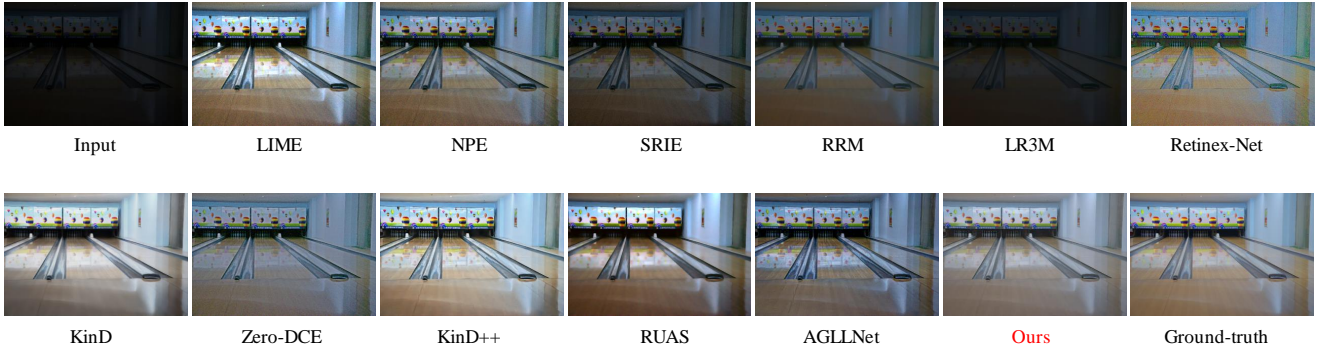


Figure 5. Visual comparison on LOL dataset #669 with SOTA LLIE methods.

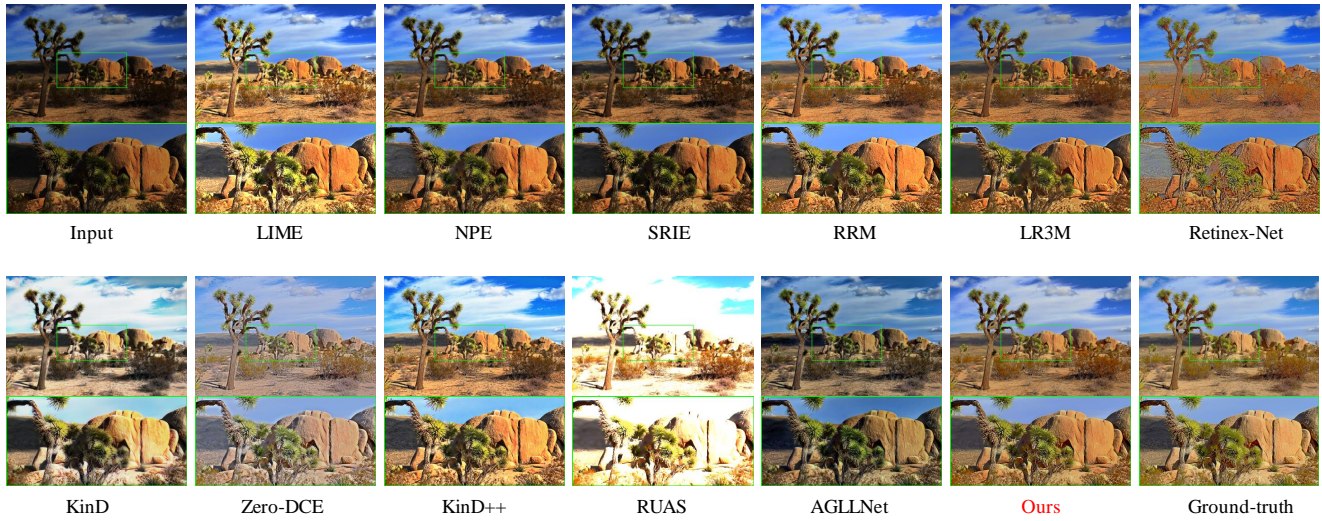


Figure 6. Visual comparison on SICE dataset #1 with SOTA LLIE methods.

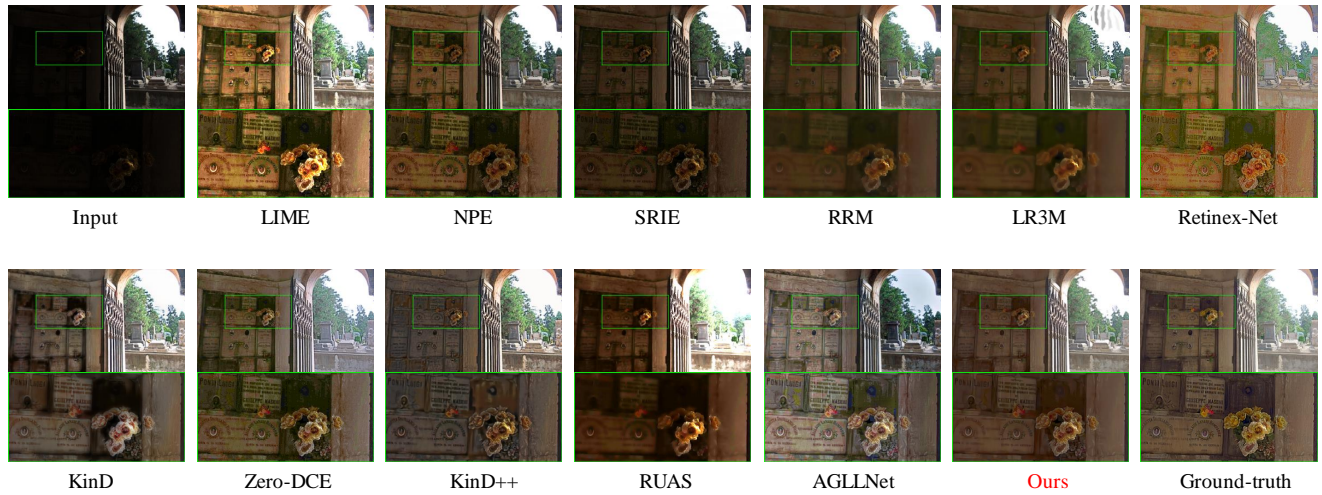


Figure 7. Visual comparison on SICE dataset #82 with SOTA LLIE methods.

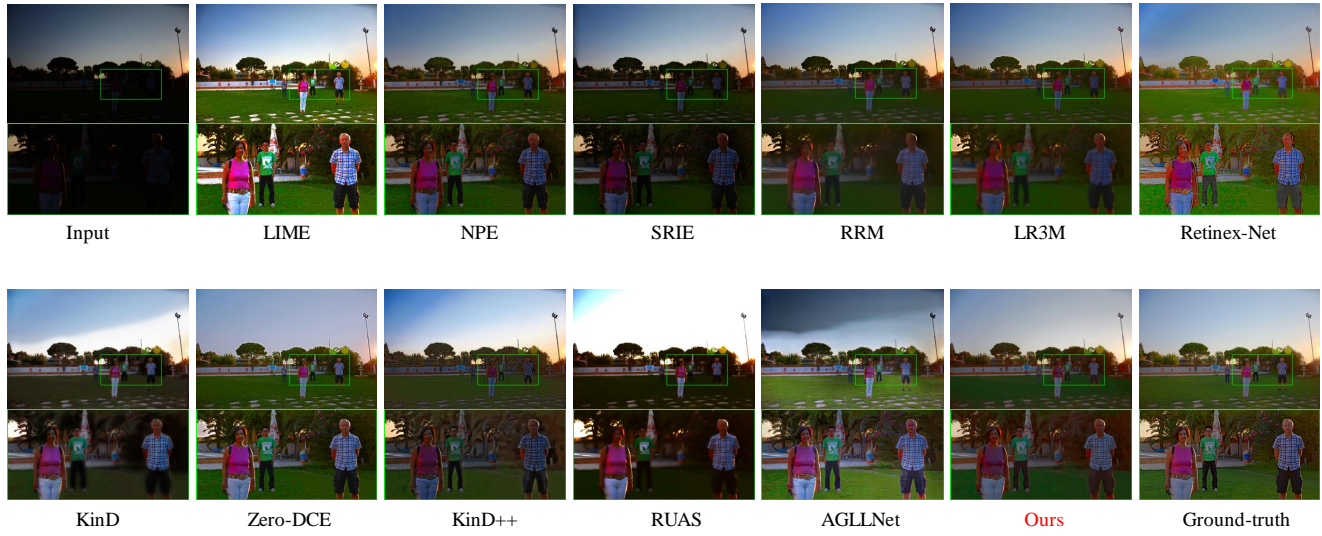


Figure 8. Visual comparison on SICE dataset #114 with SOTA LLIE methods.



Figure 9. Visual comparison on MEF dataset #Lighthouse with SOTA LLIE methods.

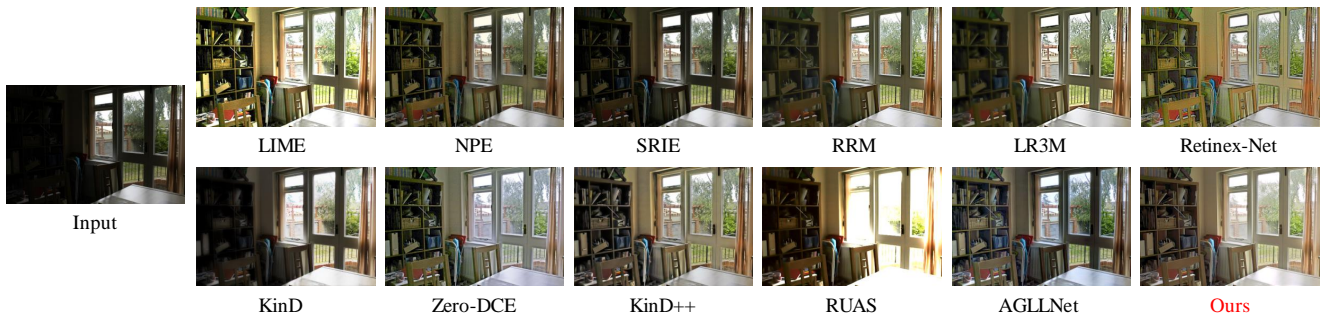


Figure 10. Visual comparison on MEF dataset #House with SOTA LLIE methods.



Figure 11. Visual comparison on MEF dataset #Venice with SOTA LLIE methods.